27th International Congress
on Sound and Vibration
The annual congress of
the International Institute
of Acoustics and Vibration (IIAV)

11-16 July, 2021

ICSV27

Annual Congress of the International Institute of Acoustics and Vibration (IIAV)

RAY-TRACING SEMICLASSICAL (RTS) PHASED GEOMETRICAL METHOD EXTENDED TO BROKEN STRAIGHT LINES TRAJECTORIES

Rok Prislan
InnoRenew CoE, Izola, Slovenia
e-mail: rok.prislan@innorenew.eu
Daniel Svenšek
Faculty of Mathematics and Physics, University of Ljubljana, Ljubljana, Slovenia
email: daniel.svensek@fmf.uni-lj.si

Ray-tracing semiclassical (RTS) geometrical method relies on the construction of the Green's function of the amplitude equation by employing the semiclassical propagator. The method is classified as a phased geometrical method capable of modeling interference effects. Nevertheless, due to diffraction, the method cannot be used in the lower frequency range for general geometries. In geometrical methods, diffraction is excluded by definition; therefore, we theoretically study the possibility of constructing the Green's function with the summation over non-classical trajectories. Broken trajectories are introduced and on this basis, an attempt is made to directly extend the RTS method to trajectories in the form of broken straight lines, which can propagate into the geometric shadow. For the free field and infinite edge cases, the frequency response is compared to the finite element method and qualitative agreement is observed. Furthermore, important aspects of the numerical implementation are presented.
Keywords: geometrical acoustics, acoustic modeling, diffraction, semiclassical methods

1. Introduction

The earliest diffraction formulations are works from Biot and Tolstoy [1] for the time-domain solution and Macdonald [2] for the frequency domain solution. Diffraction is of importance in very different scenarios, including noise barriers [3], loudspeaker enclosures [4] and performance space stage houses [5]. Diffraction is commonly perceived as the propagation of sound in shadow zones that is formed by an edge. Although this is a very prominent example of diffraction, it is a rather limited interpretation of it. In fact, in case of a barrier it is not exclusively the shadow zones that are influenced by the edge. Furthermore, diffraction is present if the angle of an edge does not divide π as a whole number, meaning it is present in most enclosed spaces. As such, diffraction is broader phenomenon as commonly perceived.

Diffraction also strongly limits the use of geometrical acoustics modeling methods (see e.g. [6] for overview), which exclude diffraction by definition. Geometrical methods are commonly extended to introduce diffraction effects as an addition to the geometrical sound field [7]. Extensions require to introduce secondary sources [8] or to split sound rays in the zone affected by the edge [9]. The approach is used for outdoor propagation [10], real-time sound propagation modeling [11] and for modeling direct sound [5]. In practice, the these methods are limited to low diffraction orders and are not used to model the whole response inside enclosures where a high number of reflections needs to be modeled. As such, in

room acoustics, geometrical modeling methods are mostly limited to the high frequency range in which diffraction effects can be neglected.

The presented approach to modeling diffraction does not rely on introducing new sources or splitting the rays, but rather by questioning the underlying assumption of geometrical methods, i.e. that straight propagation paths are sufficient to model the sound field. In our approach, the ray-tracing semiclassical (RTS) geometrical method [12] was extended to broken trajectories.

2. Theory

The ray tracing semmiclassical geometrical modeling method (RTS) has been developed [12] as an acoustic application of the semiclassical propagator emerging from quantum mechanics. The link to acoustics is the amplitude (Helmholtz) equation, which is identical for the acoustic wave equation and the Schrödinger equation.

RTS is a frequency domain phased geometrical modeling method, the main advantage of which is that it directly reproduces the Helmholtz equation Green's function G. The method has been validated in a rectangular room with a range of practically relevant boundary conditions [13], for which it is capable of precisely reproducing the fine structure of the Green's function including the room resonance frequencies and modal shapes.

3. Numeric implementation

From the technical perspective RTS is a ray-tracing method, where N sound rays propagate from the source $\mathbf{r}_0$ in random directions with an isotropic probability distribution. If a ray hits a boundary (e.g. a wall), its pressure amplitude factor changes according to the applied boundary condition while the ray specularly reflects and continues to propagate. After the amplitude of the ray reduces below a certain limit, the simulation is stopped and all rays crossing the spherical region of radius R centered at $\mathbf{r}$ are summed up.

The segments of a multiply reflected ray from the source to observation region constitute a *trajectory*, i.e., a valid connection between the source and the observation region. From these trajectories the Green's function is numerically constructed [12].

3.1 Broken RTS

Geometrical shadows are zones from which the sound source is not directly visible. It is obvious that in such case straight trajectories, on which geometrical modeling methods rely, are insufficient to model the sound field. Following Fynman's perspective [14], the sound field in shadow zones is produced by non-classical trajectories. This would mean that all possible trajectories are to be included in the model which is not possible to implement.

Therefore, we have limited our model to broken straight trajectories which would fit an arbitrary trajectory if the number of breaking points n_b would be high. As such, with the introduced approach the generality of the underlying principle has not been lost. The so introduced method has been named broken ray-tracing semiclassical (BRTS)[1].

[1]As part of our research, we have also theoretically investigated the influence of breaking points on the action of trajectories. We have derived that broken trajectories have nonstationary phase exclusively at the breaking point at which a phase integration is required. This additional step largely increases the complexity of the method and is therefore excluded from this presentation, which is in this perspective incomplete.

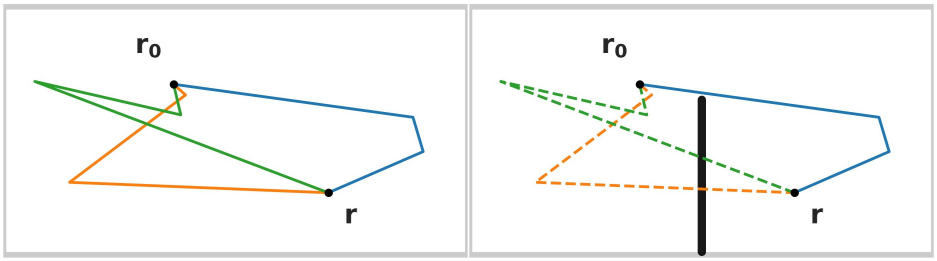

Figure 1: Graphical representation for $n_b = 2$ of three BRTS trajectories between the source and observation point. **Left:** free field. **Right:** knife-edge/vertical barrier. Broken trajectories crossing the barrier (drawn by a dashed line) are excluded from the simulation.

Trajectories between the sound source and the receiving point for $n_b = 2$ are schematically drawn in Figure 1 for the free field and knife-edge case. Trajectories crossing the barrier are identified and excluded from the simulation. This will effect the sound field to be weaker closer to the barrier.

With BRTS, N sound rays are emerging from the point source in random directions. Each ray after propagating a random straight distance brakes and continues to propagate in a new random direction. This process repeats until the number of breaking points n_b is reached.

3.2 Drawing the distance to the breaking point

The propagated distance d_i, at which the $i-$th breaking occurs, is drawn based on the exponential distribution with the probability density

$$\rho(d_i; \lambda) = \lambda \exp\left(-\lambda d_i\right), \tag{1}$$

with $\overline{d_i} = \frac{1}{\lambda}$ being the *rate parameter*. This parameter introduces the characteristic length of the system which value should not influence the obtained results.

3.3 Propagation after the last breaking point

The propagation distance from the source to the observation point is the sum of the straight sections distances

$$d = \sum_{i=1}^{n_b} d_i + d'. \tag{2}$$

d_1 is the distance from the source to the first breaking point, d_2 between the first and second breaking point etc. d' is the distance between the last breaking point and the observation point.

After n_b is reached the ray propagates in random direction and if it crosses the observation region, it would contribute to the G. A numerically improved approach for this last propagation step has been used: we let all rays contribute to G with a ratio proportional to the probability of crossing the observation region. This weighting is $\left(\arctan\left(\frac{R}{d'}\right)\right)^2$, leading to the BRTS Green's function summation

$$G_{n_b}(\mathbf{r}, \mathbf{r}_0, k) = A_{n_b} \sum_{\text{paths}} d \, \arctan^2(R/d') \, \exp\left[i\left(kd + \pi/4\right)\right], \tag{3}$$

where A_{n_b} is the normalization factor.

3.4 Normalization

With some numerical testing it was discovered that the normalization factor includes the $1/R^2$, $1/N$ and $\frac{1}{\lambda}$ dependence. Considering these the absolute pressure response has been plotted in Figure 2 in double logarithmic scale. It can be observed, that in comparison to the analytic solution, BRTS shows a $k-$dependence. The BRTS response was therefore additionally normalized following the potential function:

$$a\, b_{n_b}\, k^{K_{n_b}}. \tag{4}$$

The factors b_{n_b} and K_{n_b} are given in the legends of Figure 2. Excluding the noticeable noisy case of $\lambda = 0.05$ and $n_b = 2$, it can be seen that:

- K_1 and K_2 are relatively constant. K_1 ranges between -0.82 and -0.85, K_2 ranges between -1.53 and -1.60.
- b_1 ranges between 21 and 33, b_2 ranges between 3.2 and 6.7.

Averaging the obtained results, all further responses have been normalized using the factors of:

$$\begin{aligned} A_1 = &\quad \frac{1}{24.71}\, k^{0.83}\, \frac{1}{R^2 N \lambda}, \\ A_2 = &\quad \frac{1}{5.05}\, k^{1.56}\, \frac{1}{R^2 N \lambda}. \end{aligned} \tag{5}$$

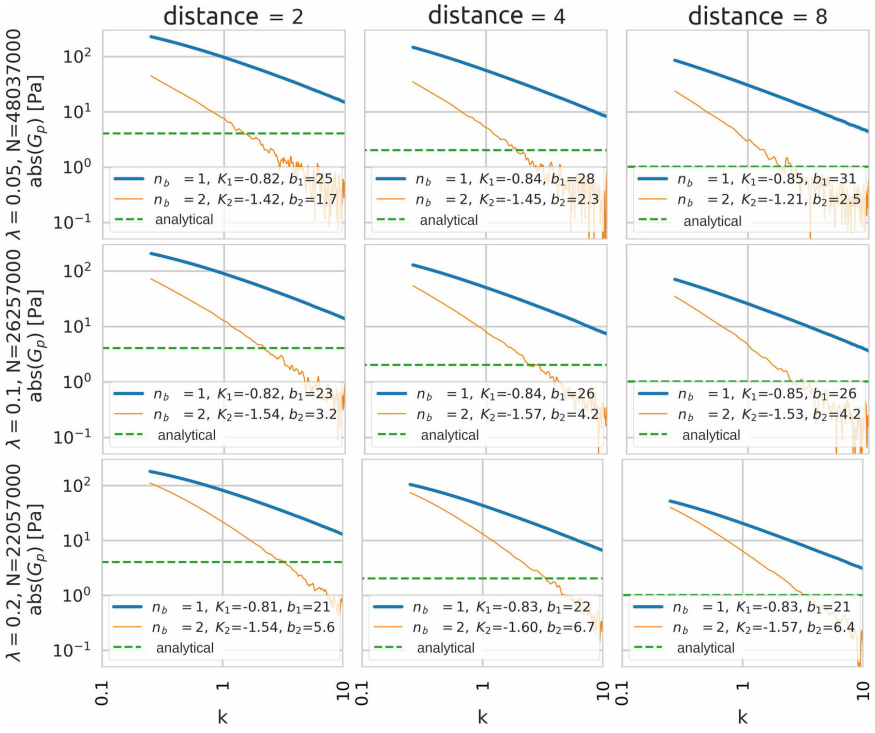

Figure 2: Absolute value of the free field pressure response generated by BRTS for $n_b = 1$ and 2 and the analytical solution. Columns correspond to different distances between the source and observation point, rows (from top to bottom) correspond to $\lambda = 0.05$, 0.1 and 0.2 (average propagation distance to the breaking point of $\overline{d_i} = 20$, 10 and 5.).

The influence of λ on the normalization was as well investigated. It has been determined that with increasing λ the k-dependence is fading. Such behavior is expected as in this case broken trajectories represent just a small extension of the classical trajectory meaning that BRTS transitions into RTS. It has been as well discovered that at small λ values the potential k-dependence becomes stationary, meaning that the normalization with a potential function is not unique for each set of simulation parameters.

4. Results

4.1 Free field

For the free field, the real values of the analytical and BRTS generated response is shown in Figure 3. The results show that:

- For the $n_b = 1$ case the amplitude and phase agreement is good.
- For the $n_b = 2$ case the BRTS response is consistent with the analytical response but contains noise.
- For the $n_b = 2$ case the noise is higher at low λ values and at higher k. This is explained by the larger variation of phase in the summation following eq. (3).
- The observed noise is of numerical nature and would reduce if N would increase.

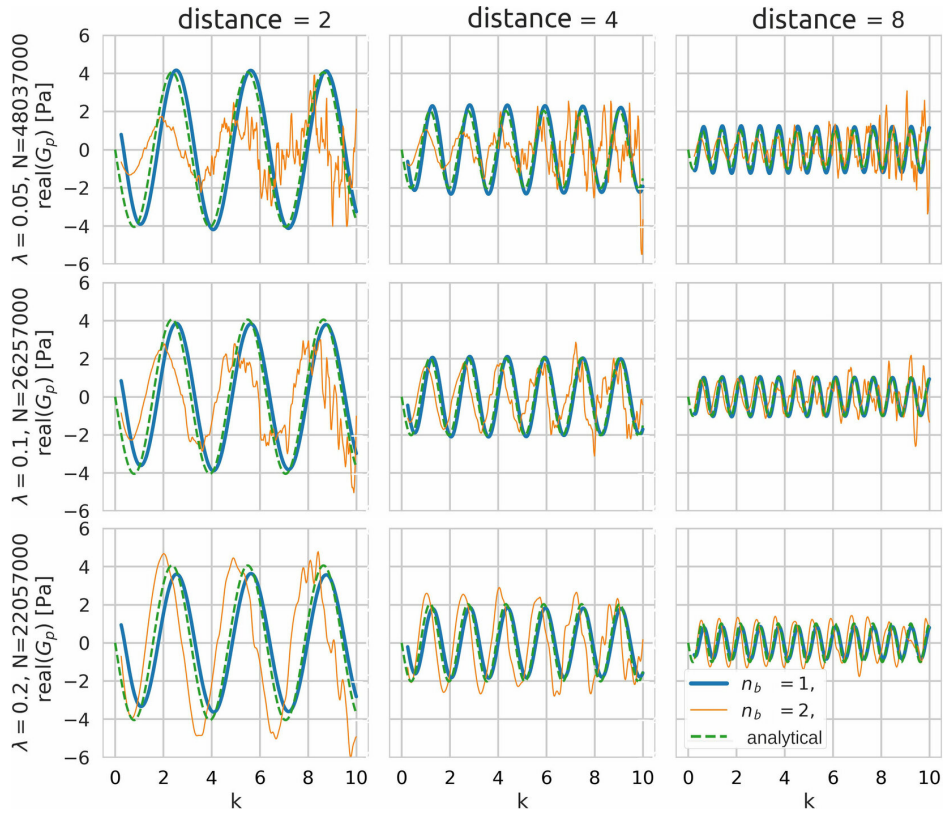

Figure 3: Real value of the free field pressure response generated by BRTS for $n_b = 1$ and 2 in and the corresponding analytical solution. The columns show the cases of source-receiver distances of 2, 4 and 8, rows (from top to bottom) represent $\lambda = 0.05$, 0.1 and 0.2.

4.2 Knife-edge diffraction

The BRTS has been tested for the knife-edge diffraction geometry[15] as graphically presented in Figure 4. Three receiving positions have been introduced, two of which in the geometrical shadow. The BRTS responses have been compared with FEM results obtained by a COMSOL implementation and are presented in Figure 5:

- The magnitudes of the BRTS responses are strongly underestimated. This is most prominent for the $T1$ case which is deeper in the geometric shadow. The $n_b = 2$ case performs better in this

perspective, indicating that more breaking points increase the chance of a valid trajectory, i.e. not crossing the barrier.

- In shadow zones the response decreases with increasing k. This dependence is more pronounced for the point $T1$ which is deeper in the shadow zone. Such trend is expected and in qualitative agreement with FEM results.
- Closer to the barrier the BRTS modeled response is weaker. Such trend is expected and in qualitative agreement with FEM results.
- For the $n_b = 2$ case a high degree of noise is observed at higher values of k.
- The phase of the responses between BRTS and FEM is in agreement. This is more evident for the $n_b = 1$, case, as for the $n_b = 2$ case high noise is present.

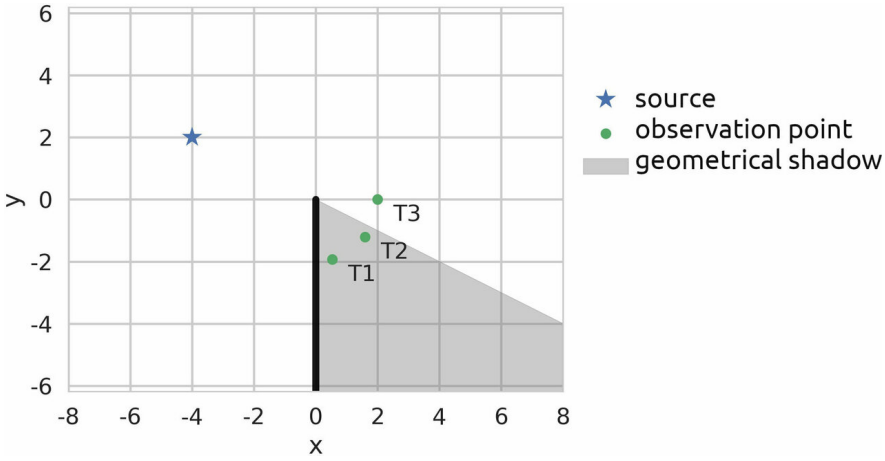

Figure 4: A cross section graphical representation of the knife-edge diffraction case: a vertical barrier, sound source and three receivers ($T1$, $T2$ in $T3$). The shaded area represents the shadow zone.

5. Conclusions

The BRTS method has been theoretically introduced and its numerical implementation presented. The normalization of the BRTS generated response on the free field case has been explained. The BRTS response has been evaluated in relation to the FEM method for the knife-edge diffraction case. Results have shown that BRTS strongly underestimates the magnitude of the response while the shadowing effect of the barrier is over pronounced. This was less prominent for the case of 2 breaking points, indicating that modeling more breaking points might improve the results. Intoducing more breaking points might increase the noise levels. It hase been as well shown, that the BRTS method correctly models the phase and frequency depended trends. This means that in case of multiple coherent source, interference phenomenon could be observed by the method.

It can be conclude that these first BRTS implementation results have shown qualitative agreement with FEM for the knife-edge case. This is a promising starting point for the further development of the method, that should include more extensive tests and a more thorough theoretical investigation of the underlying principles.

The authors gratefully acknowledge the European Commission for funding the InnoRenew project (grant agreement #739574) under the Horizon2020 Widespread-Teaming program and the Republic of Slovenia (investment funding from the Republic of Slovenia and the European Union from the European Regional Development Fund).

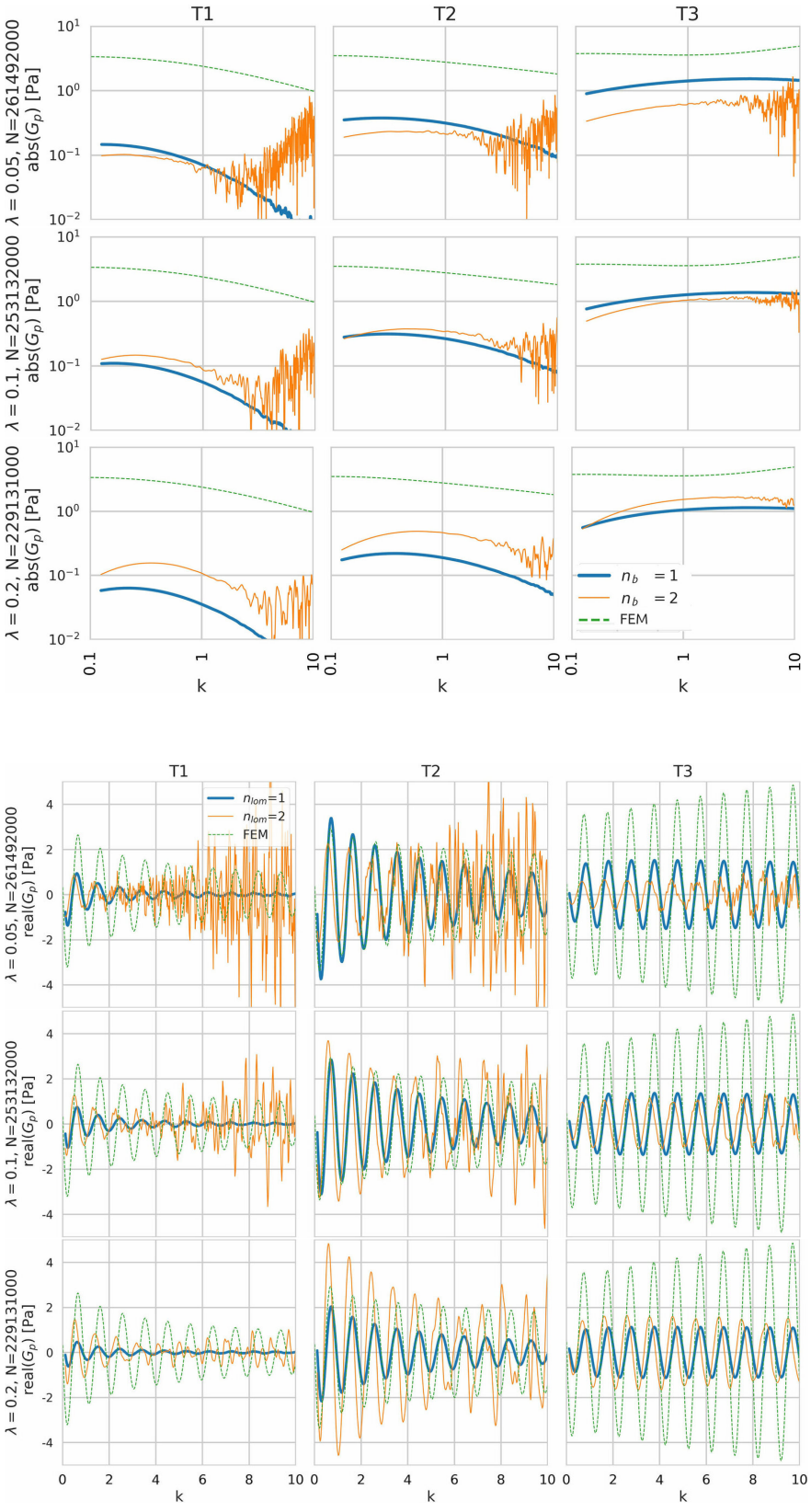

Figure 5: Pressure response obtained by FEM and BRTS for $n_b = 1$ and 2. Columns corresponds to receiving points, rows represent $\lambda = 0.05$, 0.1 and 0.2. **Top:** absolute values in double logarithmic scale. **Bottom:** real values (for convenience $T1$ in $T2$ amplitudes have been multiplied by 10).

6. List of literature references

REFERENCES

1. Biot, M. A. and Tolstoy, I. Formulation of Wave Propagation in Infinite Media by Normal Coordinates with an Application to Diffraction, *Journal of the Acoustical Society of America*, **29** (3), 381–391, (1957).

2. Macdonald, H. M. A class of diffraction problems, *Proceedings of the London Mathematical Society*, **s2-14** (1), (1915).

3. Medwin, H. Shadowing by finite noise barriers, *Journal of the Acoustical Society of America*, **69** (4), 1060–1064, (1981).

4. Vanderkooy, J. A Simple Theory of Cabinet Edge Diffraction, *Journal of the Audio Engineering Society*, **39** (12), 923–933, (1991).

5. Torres, R. R., Svensson, U. P. and Kleiner, M. Computation of edge diffraction for more accurate room acoustics auralization, *The Journal of the Acoustical Society of America*, **109** (2), 600–610, (2001).

6. Savioja, L. and Svensson, U. P. Overview of geometrical room acoustic modeling techniques, *The Journal of the Acoustical Society of America*, **138** (2), 708–730, (2015).

7. Asheim, A. and Peter Svensson, U. An integral equation formulation for the diffraction from convex plates and polyhedra, *The Journal of the Acoustical Society of America*, **133** (6), 3681–3691, (2013).

8. Svensson, U. P., Fred, R. I. and Vanderkooy, J. An analytic secondary source model of edge diffraction impulse responses, *The Journal of the Acoustical Society of America*, **106** (5), 2331–2344, (1999).

9. Stephenson, U. M. An energetic approach for the simulation of diffraction within ray tracing based on the uncertainty relation, *Acta Acustica united with Acustica*, **96** (3), 516–535, (2010).

10. Stephenson, U. M. Simulation of multiple Sound Particle Diffraction based on the Uncertainty Relation-a revolution in noise im-mission prognosis; Part I: Principle and Method, (2018).

11. Pisha, L., Atre, S., Burnett, J. and Yadegari, S. Approximate diffraction modeling for real-time sound propagation simulation, *The Journal of the Acoustical Society of America*, **148** (4), 1922–1933, (2020).

12. Prislan, R., Veble, G. and Svenšek, D. Ray-trace modeling of acoustic Green's function based on the semiclassical (eikonal) approximation, *J. Acoust. Soc. Am.*, **140**, 2695–2702, (2016).

13. Prislan, R. and Svenšek, D. Ray-tracing semiclassical (RTS) low frequency acoustic modeling validated for local and extended reaction boundaries, *Journal of Sound and Vibration*, **437**, 1–15, (2018).

14. Feynman, R. P. Space-time approach to non-relativistic quantum mechanics, *Reviews of Modern Physics*, **20** (2), 367–387, (1948).

15. Crane, R. K., *Propagation Handbook for Wireless Communication System Design*, Electrical Engineering & Applied Signal Processing Series, CRC Press, Boca Raton, USA (2003).